Experimental Mechanics (2012) 52:975–991
DOI 10.1007/s11340-011-9582-0

Multi-Scale Stereo-Photogrammetry System for Fractographic Analysis Using Scanning Electron Microscopy

M. Khokhlov · A. Fischer · D. Rittel

Received: 24 May 2011 / Accepted: 8 December 2011 / Published online: 30 December 2011

Abstract Current systems for photogrammetry analysis rely mainly on two-dimensional visualization methods, particularly Scanning Electron Microscopy (SEM). The absence of three-dimensional information prevents the determination of important quantitative features such as local roughness and precludes a deeper comprehension of the failure mechanisms. This paper describes a new multi-scale stereo-photogrammetry system for inspection of fracture surfaces based on SEM images. The system facilitates the reconstruction of complete 3D fracture surfaces and provides interactive visualization of the multi-scale structure, thus offering better insight into fracture surfaces at different levels of detail. In particular, a new method has been developed for geometric reconstruction of a 3D textured mesh from SEM stereo images. The mesh is represented as a 3D geometric multi-resolution structure. The sampled images are represented in the form of a multi-scale hierarchical textured structure. Thus, the global shape of the sample is represented by a 3D mesh, while its micro details are represented by textured data. This multi-scale and hierarchical structure allows interactive multi-scale navigation of the 3D textured mesh. The Regions of Interest (ROI) can actually be inspected interactively at different scales by means of *optical* or *digital zooming*. Thus, the digital model can be visualized and the behavior of the 3D material can be analyzed interactively. The contributions of this research include: (a) a new 3D multi-scale reconstruction method for SEM stereo images; (b) a new visualization module for multi-scale inspection, modeling and analysis of micro-structures for a variety of materials; and (c) 3D insight into and better understanding of fracture phenomena for material micro-structures. The feasibility of the proposed method is demonstrated on samples of different materials, and a performance analysis is applied on the resulting multi-scale model. The roughness calculation was verified against roughness calculation applied to the optical profilometer.

Keywords Fracture surfaces · Stereo-photogrammetry · Multi-scale · Multi-resolution · Textured meshes · Visualization analysis

M. Khokhlov · A. Fischer (✉)
CAD & LCE Laboratory, Faculty of Mechanical Engineering, Technion,
Haifa 32000, Israel
e-mail: meranath@technion.ac.il

M. Khokhlov · D. Rittel
Materials Mechanics Center, Faculty of Mechanical Engineering, Technion,
Haifa 32000, Israel

Introduction

F*racture mechanisms* have been examined and studied for about two centuries in an attempt to optimize the toughness of engineering materials. Over the years, techniques for assessing fracture surfaces have evolved considerably, particularly with the development of microscope technologies such as *Scanning Electron Microscopy (SEM)*. Today, high magnifications at high resolutions enable scientists and engineers to visualize fracture surfaces at a resolution of 1–20 nm that allows for detailed assessment of the toughening vs. weakening failure micro-mechanisms. Nevertheless, very few research studies have utilized fracture images to generate full 3D textured surfaces with multi-scale geometric representation. Moreover, utilizing a multi-scale approach for analysis of fracture surfaces overcomes the difficulty of acquiring high resolution images that cover the entire area of a surface. With this approach, lower resolution images can

represent an entire area, while high resolution images represent only a few Regions of Interest (ROI). The availability of full 3D pictures can pave the way for the assessment of quantitative features such as local roughness on a large spatial scale, a capability that is currently unavailable. Moreover, such images can provide better qualitative comprehension of the crack path and its relation to the micro-mechanisms of failure.

This paper describes a new multi-scale stereo-photogrammetry system for inspection of fracture surfaces from SEM images. It includes a new method for modeling fracture surfaces that reconstructs 3D multi-scale textured meshes. The resulting model allows better understanding of a fracture surface and its material characteristics. The method incorporates knowledge and algorithms from interdisciplinary fields, e.g. stereo-photogrammetry, multi-resolution mesh reconstruction, texture mapping and multi-scale analysis. The state of the art for these techniques is described in the following section.

Overview

Multi-scale Material Structure

Materials are characterized by complex multi-scale structural geometry and complex behavior and exhibit different architectures at different levels of hierarchy [1, 2]. In the micro-structures of fracture surfaces, the material architecture and texture differ significantly with respect to shape, texture and direction, depending on the surface site. Moreover, due to heterogeneous characteristics, the mechanical properties of a material may vary significantly at different micro-scale levels, even in a small area. Therefore, visualization of 3D multi-scale micro-structures can serve as a basis for analyzing the behavior and exploring the properties of different materials. The following section summarizes various visualization techniques.

Visualization of 3D Multi-Scale Micro-Structures

Fracture Surface Analysis Surface roughness, a common mechanical property, can be analyzed either via different material cross-sections or through statistical analysis of the entire tested sample area. One of the state-of-the-art methods for profile analysis is the FRASTA method [3], which makes it possible to analyze the mechanical behavior of a surface through a predefined profile. Nevertheless, the lack of explicit 3D information requires assumptions and interpretations about the missing data. A significant advance in surface analysis [4] focuses on 3D reconstruction of fracture surfaces. However, this method reproduces only a global shape of the surface, and ignores the fine details of the fracture surface. Therefore, a method that includes simultaneous representation of global features and fine details is needed for reconstructing textured meshes from SEM images.

Stereo-Matching on SEM Images Several methods can be used to generate stereo-photogrammetry of 3D fracture surfaces from SEM images [3–9]. These 3D reconstruction methods can be used to extract profiles and examine roughness, local toughness, fracture energy and critical crack tip opening. This approach has provided good results for complex textures characteristic of fracture surfaces. In this paper we apply matching on SEM images to find the best similarity between patterns (Fig. 3(b)).

Reconstruction of 3D Meshes Stereo-photogrammetry yields a cloud of 3D points from which a mesh is reconstructed [10, 11]. Mesh construction can be difficult, especially in complex real 3D cases where the resulting mesh is not unique and well defined [12, 13]. Nonetheless, because stereo-photogrammetry is a 2.5D problem, an object can be projected in 2D without loss of information. Thus, meshing is much simpler than in 3D and can be handled as a terrain mapping problem [14]. The two classical meshing approaches are Delaunay triangulation [15] and grid-based meshing [16]. In the current study, a grid-based method is used to reconstruct the quad mesh.

Texture Mapping on Meshes Texture mapping, required for realistic visualization of 3D surfaces, involves applying a 2D textured image on the reconstructed 3D mesh. Texture mapping, one of the leading techniques in high quality image synthesis [17], can enhance the fine details of scan images while requiring only a relatively small increase in computation. Mapping a 2D texture onto a 3D surface requires parameterization of the polygonal mesh [11]. In the proposed method, a given image of the micro-structure surface is mapped on the 3D mesh to yield a 3D representation. Though texture mapping is considered a complex problem, in this case the problem is simplified because the geometry of the samples has 0-genus and is 2.5D. The resulting textured mesh contains both global information of the 3D shape and fine micro structure details.

Multi-Scale Modeling Multi-scale modeling is applied in mechanical computations such as finite element analysis to create models with more details and to acquire information at previously unavailable scales and sub-scales. The use of a multi-scale approach for analysis of fracture surfaces overcomes the time and space complexities of acquiring high resolution images for an entire surface area of the sample. Lower resolution images are acquired for the entire area, while high resolution images are used only for a few

Regions of Interest (ROIs) that can be changed dynamically in space and scale. In this study, the entire model is initially reconstructed and visualized at a lower scale level. When a higher scale is required for specific ROIs, the system seamlessly switches to a higher resolution model. In cases where high resolution information partially overlaps the ROI area at the lower resolution, a fusion of different resolutions can be visualized.

Multi-Resolution Geometric Data Structure The multi-resolution approach is used for decomposition of geometric models at hierarchical levels of details [18]. A multi-resolution representation comprises a hierarchy of intermediate geometric models. This approach facilitates: (a) rapid model compression and simplification; (b) fast, progressive and view-dependent rendering; (c) data transmission; and (d) level of detail control. The method described in [19] utilizes a Hierarchical Space Decomposition Model (HSDM) based on an octree data structure [20], where the set of original points in each voxel is replaced by a representative vertex that is later used for connectivity graph calculation and further mesh reconstruction. The position of the representative vertex is defined as a centroid of the sampled points for each cell, and the operation can be considered as low-pass filtering of the input data. Thus, the process becomes more robust and stable with respect to sample noise. The HSDM resolution can be changed during visualization, showing the scanned sample at different levels of details. As the resolution becomes lower, reconstruction and visualization get faster.

Multi-Scale Texture Mapping Similar to one-scale texture mapping (section 2.3), multi-scale texture mapping is required for realistic 3D surface visualization of the reconstructed multi-scale mesh [21]. For an ROI that is directly reconstructed from scanned SEM images, the texture is defined by one of these images. In cases where an ROI is calculated from 3D meshes at a lower scale, digital zooming is applied and the texture is up-scaled according to the required ROI resolution.

Multi-Scale Material Analysis Material properties analyses are used to examine the multi-scale surface behavior of the explored material [22]. Surface roughness can be analyzed either through different material cross-sections or by statistical analysis of the entire tested sample area. For some materials, surface architecture and texture differ significantly at different scales with respect to shape, texture and directionality. Therefore, a multi-scale structure is crucial for analyzing material behavior and exploring material properties at different sites and different scales.

Approach

The objective of this research has been to develop an automatic 3D system for inspection that creates multi-scale models from SEM stereo images. A schematic representation of the proposed system is depicted in Fig. 1. The feasibility of the system is demonstrated on several fracture surfaces scanned by a SEM.

The proposed algorithm is based on the following stages:

a. Reconstructing a 3D multi-resolution mesh with multi-scale texture. The reconstruction algorithm is applied on stereo images at different scales from a variety of sites to compute the 3D clouds of points and reconstruct the 3D ROIs meshes. Then, a multi-resolution mesh is computed that integrates the ROIs meshes. Finally, multi-scale texture mapping is applied on the multi-resolution mesh.
b. Generating intermediate levels in the hierarchical structure.
c. Navigating via the scales and visualizing the fracture surface at different ROIs. The multi-scale textured mesh enables visualization of the surface behavior at different scales. Moreover, the user can interactively select ROIs by zooming in/out interactively. The zooming can be optical or digital.

The proposed SEM-based inspection system allows automatic and high-precision inspection of fracture surfaces at sub-micro

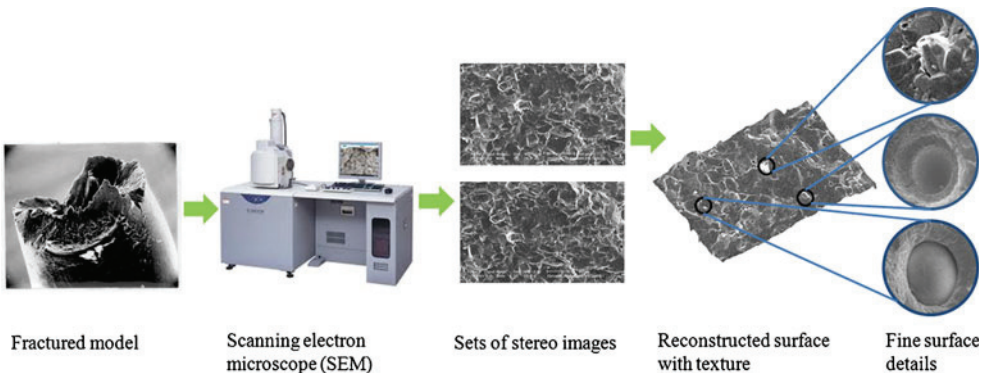

Fig. 1 The proposed system for multi-scale stereo-photogrammetry inspection of fracture surfaces

levels to provide material and mechanical engineers with improved understanding of fracture phenomena and feedback. The inspection process is demonstrated in Fig. 2.

In this paper, the proposed multi-scale method has been evaluated as follows:

Stage 1 SEM stereo image acquisition

Sets of stereo images are sampled for reconstructing the 3D meshes. These sets include different materials in order to test system robustness and performance.

Stage 2 Calculating the correlation between patterns - the matching process

Stereo images are processed to detect pattern similarities, thus providing the basis for matching [23] each individual pixel in the SEM images acquired in previous stage. In our system, each pixel is represented by a region that includes it. Similarity between the representative regions is calculated. Three main parameters were used in this process: pattern-window, searched window and features location on SEM image (Fig. 3). The resulting data represents the 3D surface points.

Stage 3 Calculate the meshes from the 3D points

Once 3D surface points have been created for each individual scale, 3D meshes are calculated out of these 3D points. Then, the texture has been applied to each created mesh. The texture is needed in order to receive visually realistic-looking surfaces.

Stage 4 Reconstruction of 3D multi-scale model

A hierarchical multi-resolution model is reconstructed from the resulted meshes. The resulted meshes are represented in a hierarchical grid-based data structure, e.g. octree [20]. Stereo images for different scales are stored in a hierarchical multi-scale data structure. The images are mapped onto the multi-resolution mesh using texture mapping.

The feasibility of the proposed inspection method is demonstrated on sets of SEM stereo images taken for different materials and at various regions of interest. The inspection system has been tested for robustness, sensitivity to different fracture surfaces and degree of detail on the textural and structural levels. Fractography experts can use the interactive interface to analyze the performance of the multi-scale inspection system. This analysis module includes verification of reconstruction, quality and precision, multi-scale system behavior and detection of fine details.

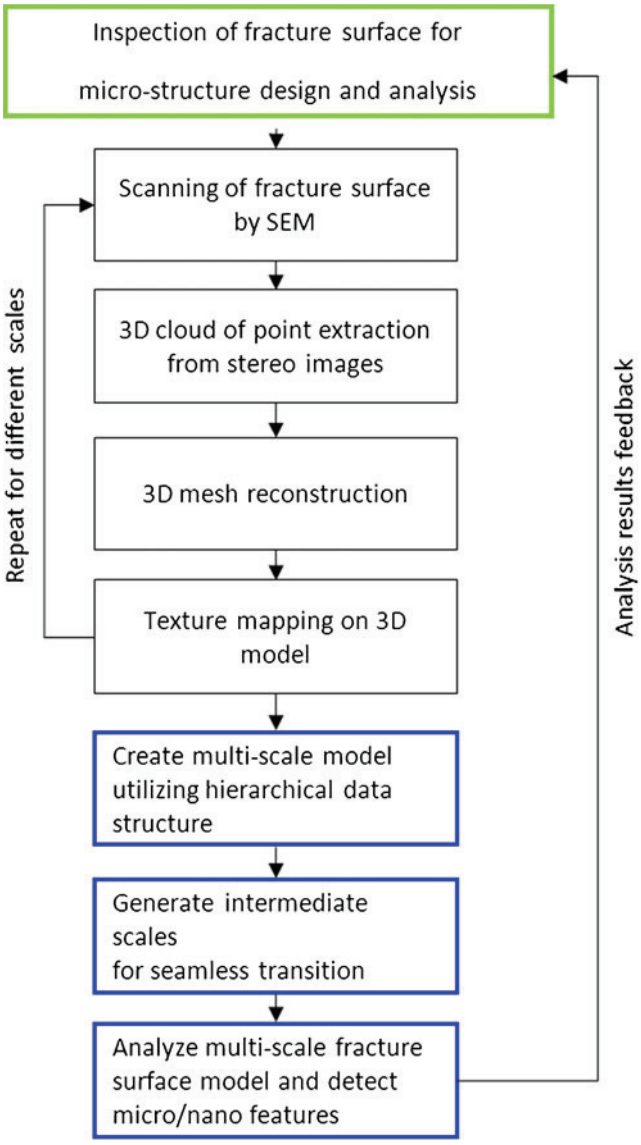

Fig. 2 Proposed inspection system from SEM images

Implementation

The implementation stage includes the following steps:

a. Extracting 3D points from stereo images.
b. Computing 3D meshes from the SEM stereo images.
c. Texture mapping of the images on the resulting meshes.
d. Multi-scale modeling of fracture surface.

Extracting 3D Points from Stereo Images

3D points are extracted from stereo images by applying stereo matching [24]. The stereo images are defined as the

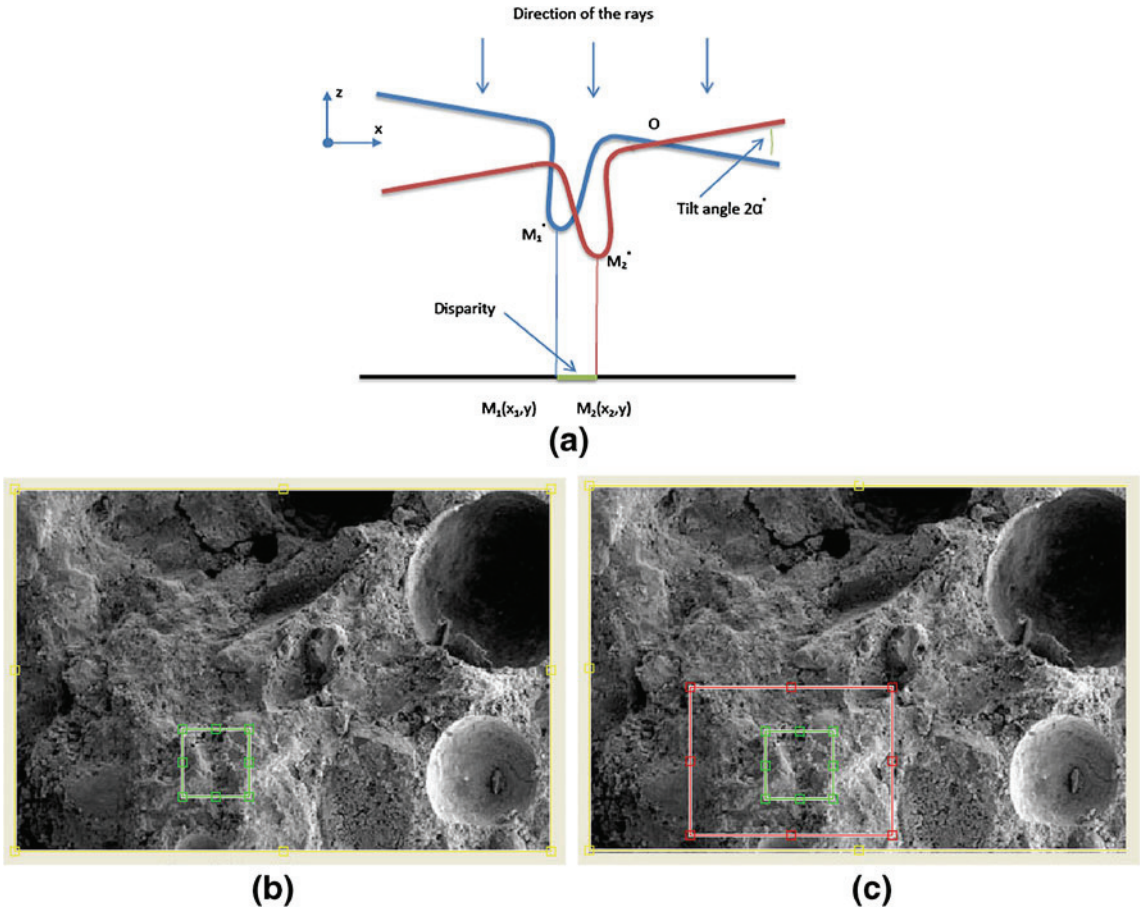

Fig. 3 The stereo matching on *earth magma* material: (**a**) and two SEM images (**b**)–(**c**) with marked matching features-*pattern-window* denoted by green frame within the *searched-window* denoted by red frame

source image and the *target image*. A *pattern-window* of the *source image* is defined according to texture behavior, i.e. levels of detail and irregularity. *The pixel of interest* is located in the middle of the *pattern window.* Features with a high level of detail are correlated to a small *pattern-window.* Increasing the window size produces a higher level of smoothing and matching, which is less accurate and less sensitive to sharp changes in the surface. The *searched-window* of the *target image* contains the *pattern-window,* and therefore should be larger than the *pattern-window* and also defined according to the texture behavior.

In pattern recognition, *cross-correlation* is a measure of pattern similarity between a *template* and an image. In our case, the *template* is defined as the *pattern-window,* while the image as the *searched-window.* The cross-correlation will be high where the *template* and *image regions* are highly similar. The cross-correlation algorithm for images is described in [25, 26]. We used Matlab R2009a [27] for calculating the cross correlation. The time complexity of the cross-correlation algorithm is $O(n^2)$, where n^2 is the number of *template pixels*. Therefore the template should be as small as practicable. For image-processing applications in which the brightness of the image and template can vary due to lighting and exposure conditions, the images can be first normalized.

Figure 3 schematically depicts the reconstruction process. The matching features *pattern-window* is denoted by a green frame within the *searched-window*, denoted by a red frame (Fig. 3(b) and (c)). These parameters are important for the matching process. Point M has two projections (M_1 and M_2) from two different directions of projection (or "view"). If these two points and the angle 2α between the views are known, computing the depth "z-value" of point M is straightforward. In the scanning process, the tilt axis should be located in the middle of the image to minimize image aberrations and distortion effects. Otherwise, the aberrations produced by SEM scanning should be taken into consideration during stereo matching computation. The output is a cloud of 3D surface points [11].

The normalized cross-correlation function is defined as follows:

$$\gamma(u,v)=\frac{\sum_{i=u-N/2}^{u+N/2}\sum_{j=v-N/2}^{v+N/2}\left[Image_{i,j}-\overline{Image_{u,v}}\right]\left[Template_{(i-u,j-v)}-\overline{Template_{u,v}}\right]}{\left\{\sum_{i=u-N/2}^{u+N/2}\sum_{j=v-N/2}^{v+N/2}\left[Image_{i,j}-\overline{Image_{u,v}}\right]^2\left[Template_{(i-u,j-v)}-\overline{Template_{u,v}}\right]^2\right\}^{0.5}}$$

here

- $\overline{Image_{u,v}}$ is the mean of *the image* in the region that overlaps the *template*
- $\overline{template}$ is the mean of the template
- *N–Template size*

Reconstruction of a Mesh from Cloud of Points

Mesh reconstruction is difficult, especially in complex real 3D cases where triangulation is not unique and well defined [12, 28]. Nonetheless, because stereo-photogrammetry is a 2.5D problem, an object can be projected in 2D without loss of information, and the meshing can be handled as a terrain mapping problem [14]. Figure 4 depicts reconstruction of the quad mesh.

In the case of outliers, filtering is applied on the 3D mesh. As a result, isolated sharp peaks are eliminated, and the mesh is smoothed and assumes the behavior of a topographic map. The filtering process is demonstrated in Fig. 5.

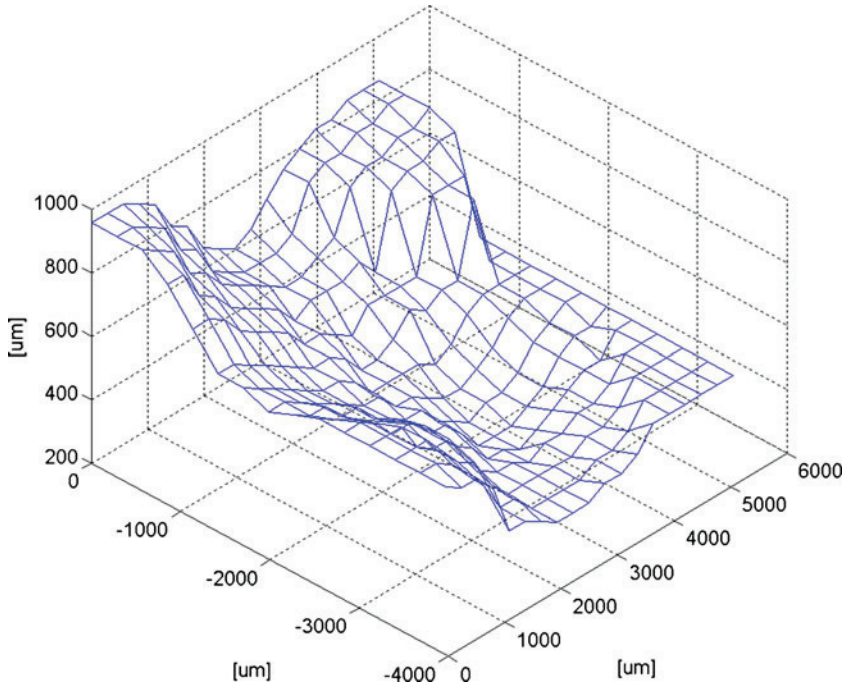

Fig. 4 A quad mesh reconstructed from 3D points

Texture Mapping on a Mesh

After the 3D mesh is reconstructed, the image of the micro-structure surface can be mapped to form a 3D representation of the textured mesh. The new 3D model contains both global information about the 3D shape and fine details of its micro-structure in the form of texture. Figure 6 shows an example of a reconstructed fracture surface, Fig. 7 depicts the surface of biological material and Fig. 8 illustrates a fracture surface for high purity alumina material.

Multi-scale Modeling of Fracture Surface

The reconstruction process is applied on each sampled region scanned by a SEM, and a 3D mesh is created for each ROI. The ROIs are defined in a variety of sizes, sites and scales according to material analysis requirements. After that, the multi-scale meshes are integrated into a single multi-resolution mesh. Intermediate levels can be calculated for regions in which the transition between two consecutive levels is not sufficiently smooth. Such intermediate levels

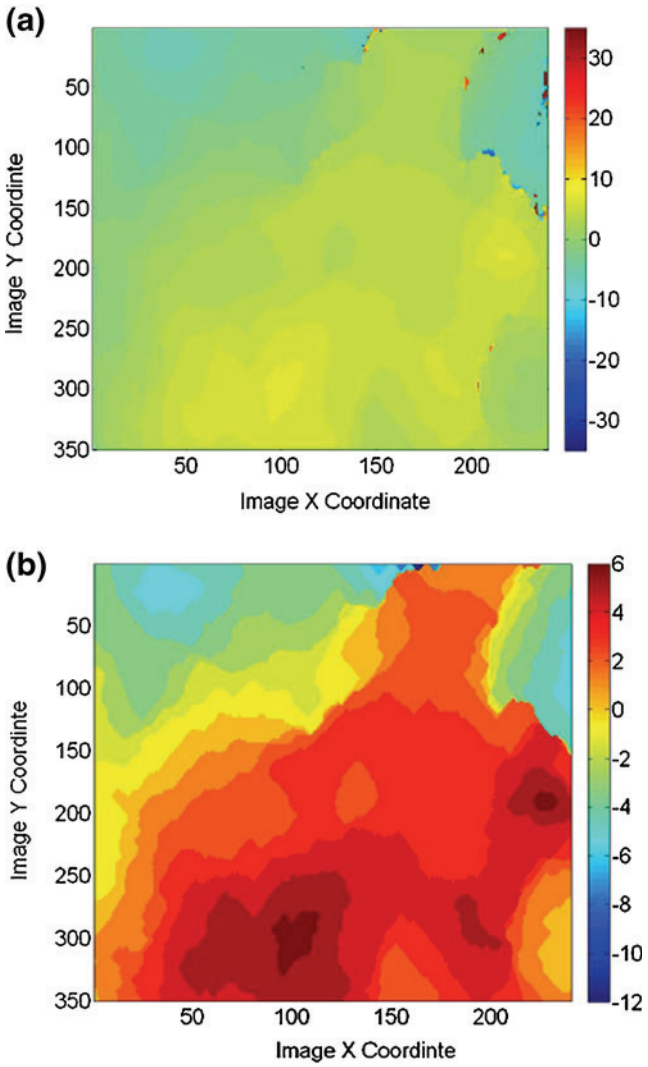

Fig. 5 A colored depth map of the mesh: (**a**) with outliers; and (**b**) after filtering and smoothing

are processed as digital reconstructed scale levels (analogous to *digital zooming*) and are an inherent part of the multi-resolution mesh. In our system a hierarchical multi-resolution structure in the form of a tree has been defined. The multi-scale concept and an example are depicted in Figs. 9 and 10.

The main stages of the multi-scale *zooming-in* operation are as follows:

- Mark the *zooming-in area* and the *zooming-in magnification*.
- For each ROI that is included in the *zooming area*:
  - If the *ROI magnification* is higher than or equal to the *zooming magnification*, replace the mesh of the ROI with the current mesh, in the overlapped area.
  - Otherwise, apply the digital *zooming-in* to the *zooming magnification.*

The main stages of the multi-scale *zooming-out* operation are as follows:

- Mark the *zooming area* and the *zooming-out magnification*.
- For the minimal ROI that contains the *zooming area*:
  - If the *ROI magnification* is lower than or equal to the *zooming magnification*, replace the mesh of the ROI with the current mesh, in the overlapped area.
  - Otherwise, apply the digital *zooming-out* to the *zooming magnification.*

The resulting structure is composed of meshes at different resolutions. The algorithm should preserve C1 continuity.

Profile Analysis

Profiles contain explicit information (e.g. roughness) about the physics of the fracture. A profile can be computed in any desired direction to analyze the roughness of a surface. The profile is obtained by computing the intersection of the surface with a given plane. Its curvature can then be analyzed, and subsequently the profile itself can be analyzed. Extracting a profile from a surface is straightforward in our case because the surface is in 2.5 dimensions. Figure 11 shows an example of profile extraction following a specific direction.

Examples and Performance Analysis

The proposed method has been demonstrated on several samples. The performance of the resulting multi-scale model has been analyzed for each sample on each scale separately.

In the examples, we decided to compromise by using the smallest tilt angle possible to process the data (5 deg is adequate for that purpose), since larger angles will result in a loss of focus and/or depth of field. While this can be corrected on most SEMs, we did not want to induce this kind of optical preconditioning to the raw data.

The Error Functions

The following error functions were evaluated:

a. Depth error (z value) with respect to tilt angle;
b. Depth error (z value) with respect to image disparity:

The following parameters are defined:

- The tilt angle α [in radians].
- The pixel disparity *Pixel_disparity* [in pixels].
- The pixel size *Pixel_size* [in mm].

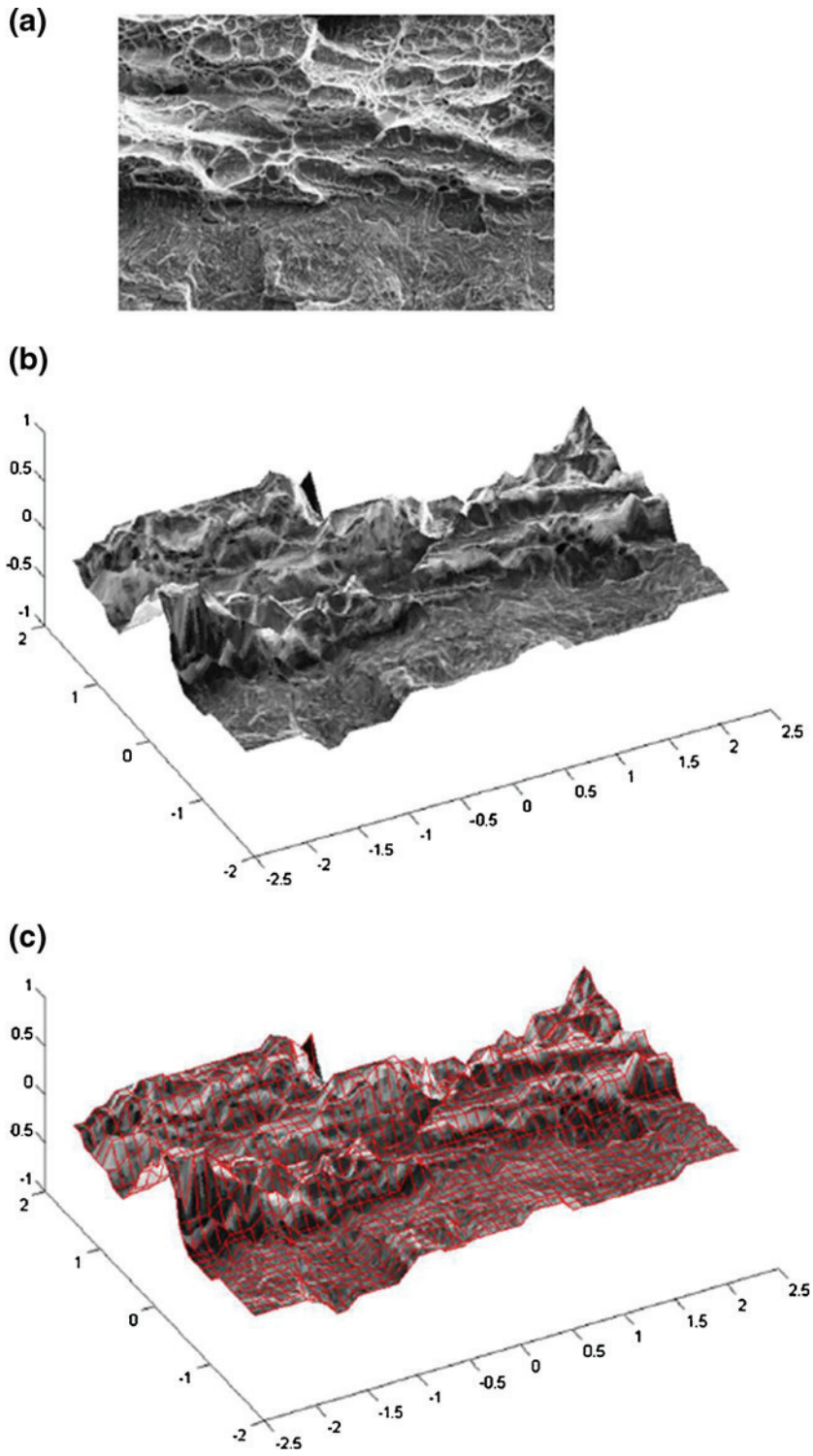

Fig. 6 Reconstruction of the model: (**a**) the SEM image. (**b**) 3D textured-mesh; and (**c**) the quad mesh (arbitrary units)

- The height Z_{ij} of each computed 3D point P_{ij} [in mm].
- The height error δz [in mm]

Depth error with respect to tilt angle:

Z_{ij} can be computed from the following equation:

$$Z_{ij}(\alpha) = \frac{Pixel\_disparity_{ij} \cdot Pixel\_size}{2 \sin \alpha}$$

Then the δz can be calculated:

$$\delta z(\alpha) = \frac{Pixel\_disparity_{ij} \cdot Pixel\_size}{2 \sin \alpha \tan \alpha} \delta\alpha$$

$$\varepsilon_z = \frac{\delta z}{z} = \frac{\delta\alpha}{\tan \alpha}$$

In our case, α=5° and $\delta\alpha$=0.5° (8.73e–3[rad]).

Substituting in the above equations, the height error ε_z is 10%.

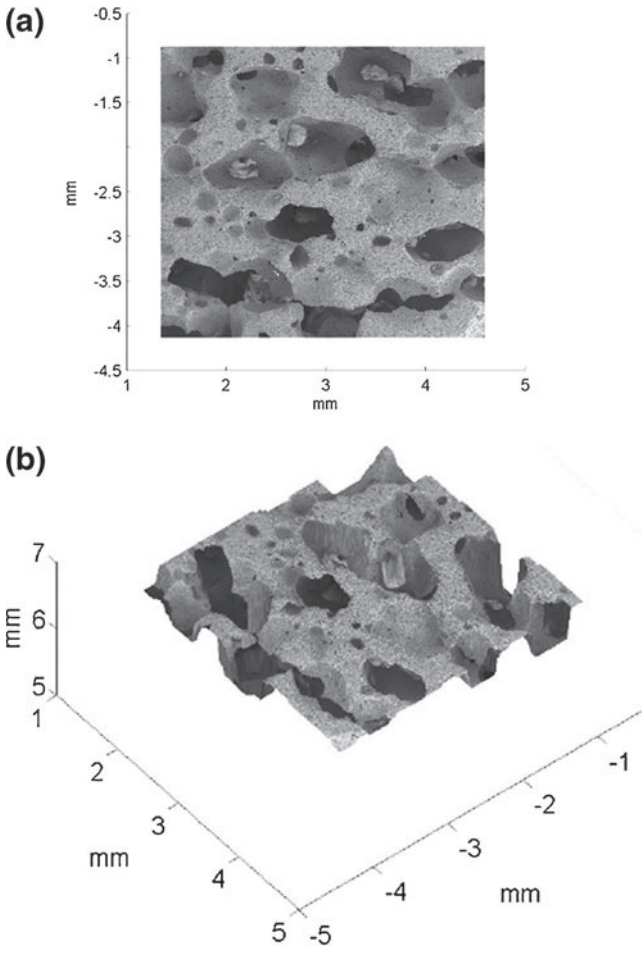

Fig. 7 Biological material (X18): (**a**) SEM image; (**b**) the reconstructed surface

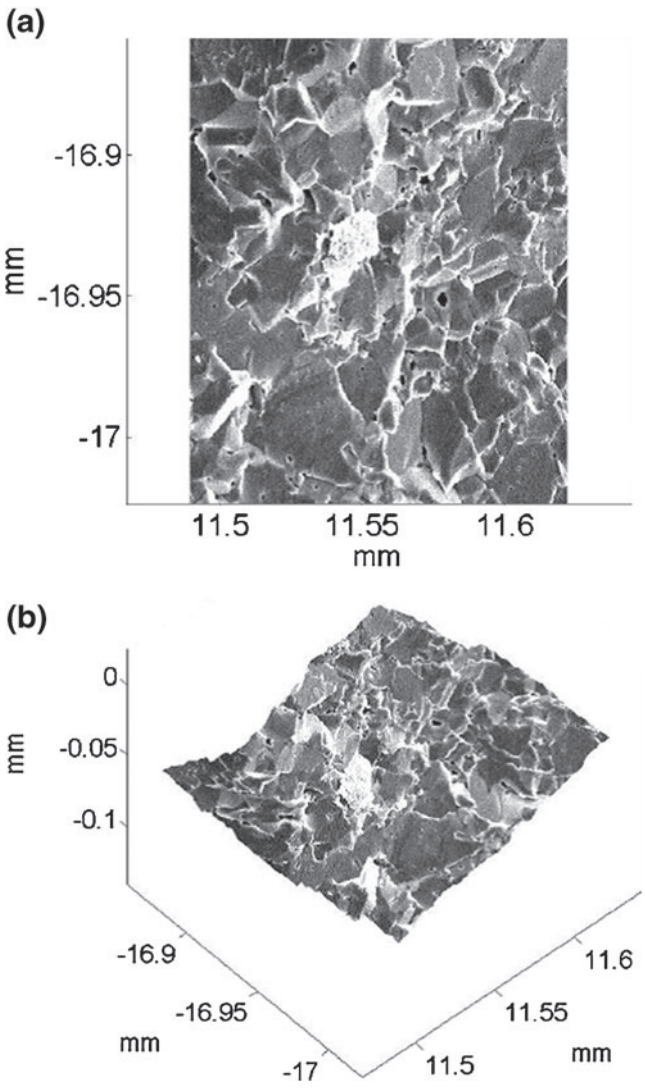

Fig. 8 Fracture surface of high purity alumina (X800): (**a**) a SEM image; and (**b**) 3D surface

Depth error with respect to image disparity:

The disparity error resulting from image resolution is assumed not higher than one pixel. Due to different tested scales used in fracture SEM analysis, typical *pixel-size* values vary between 1 μ/pixel and 0.005 μ/pixel. Typical *tilt angle* is ±5º. Therefore the depth error is given as follows:

$$0.03\mu \leq \delta z(Pixel\_disparity) \leq 5.7\mu$$

The low boundary of the depth error relates to the high scale (0.005 μ/pixel) and the high boundary of the depth error relates to the low scale (1 μ/pixel). It is important to note here that the distortion error caused by SEM imaging system was disregarded.

Examples: Multi-scale Textured Mesh

The proposed multi-scale approach was tested on several material samples, and the fractographic images were generated at different scales. Samples of *ductile broken steel* and *brittle material* were scanned at zooms of x800, x1600 and x3200. The dark areas refer to the optical zooming of the SEM, while the light areas refer to the digital zooming.

Figure 12 shows the images for *ductile steel*, with a smooth transition between the areas of the optical and the digital zooming. As expected, the optical zooming provides more details than the digital zooming. The features can be identified clearly at different scales.

Figure 13 presents the 3D textured meshes for *ductile steel*. In 3D as well, there is a smooth transition between the areas of the optical and digital zooming, though this is not guaranteed and should be handled in the future by the reconstruction algorithm that integrates the multi-scale meshes. The 3D features can be identified clearly at different scales.

Figure 14 presents the typical fracture surfaces and the corresponding 3D textured meshes for *ductile steel* at a zoom of x3200. The meshes (red lines) are shown on the

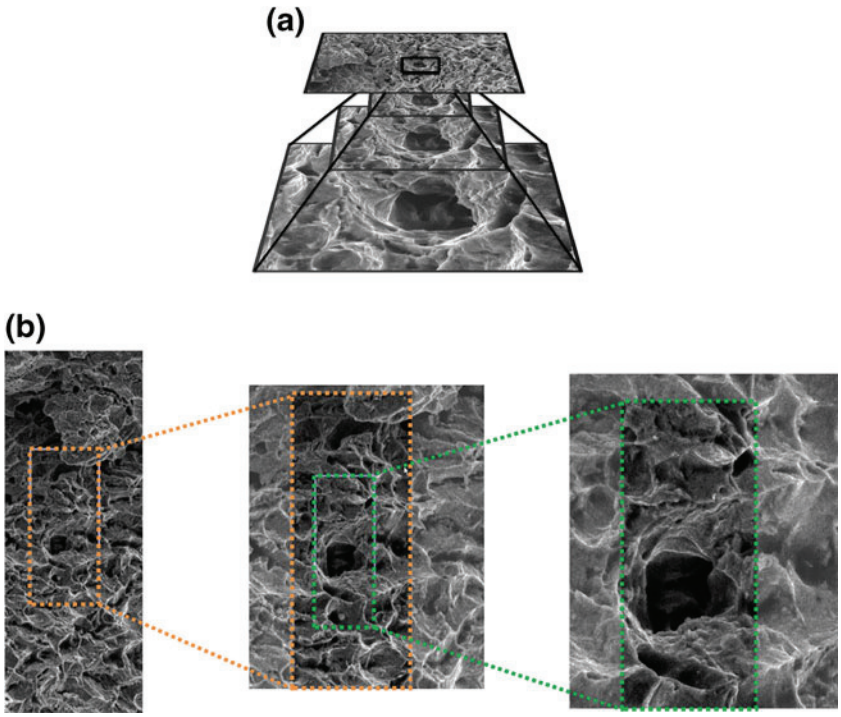

Fig. 9 Hierarchical image data structure: (**a**) tree concept; (**b**) image-based multi-scale representation of fracture surface. Dashed window depicts the selected Region of Interest (ROI)

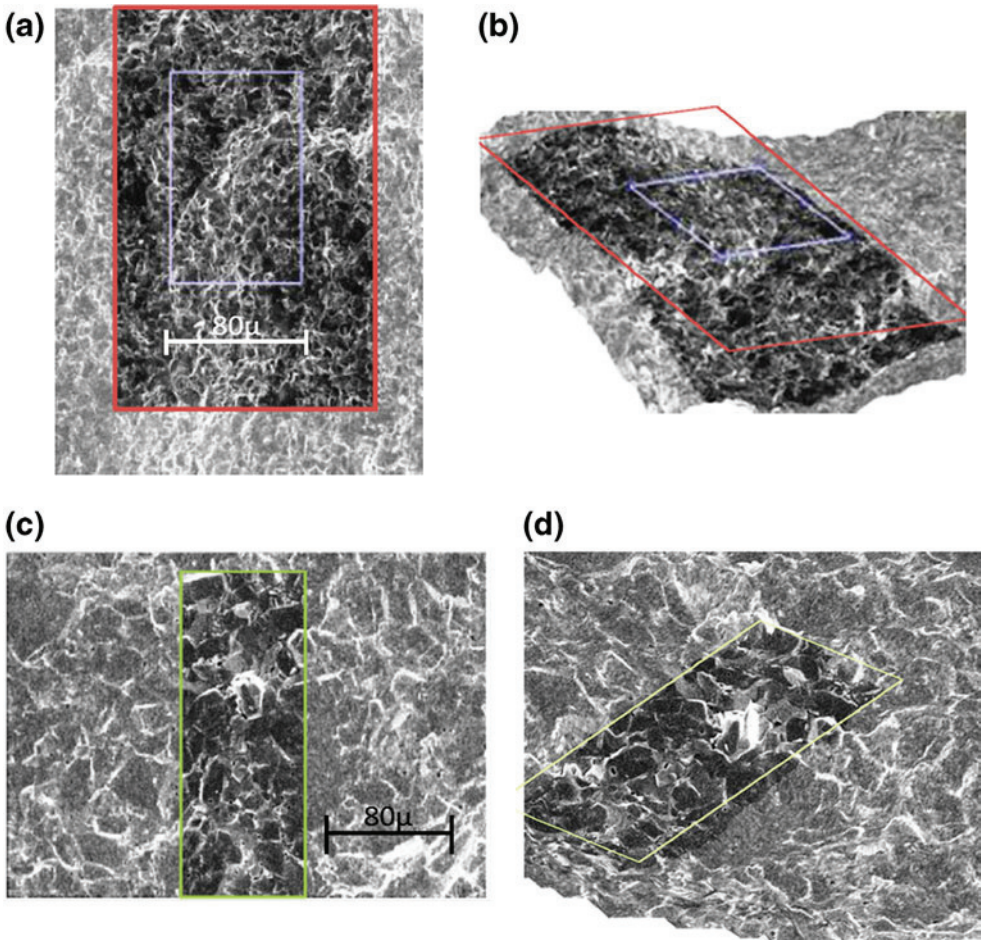

Fig. 10 Multi-scale representation of 3D fracture surface of high purity alumina material: (**a**) top view of high-magnification (X200)- (selected ROIs) and low-magnification (x100)- textured meshes; (**b**) 3D of high-magnification (X200)- (selected ROIs) and low-magnification (X100)- textured meshes; (**c**) top view of high-magnification (X400)- (selected ROIs) and low-magnification(X200)- textured meshes. (**d**) 3D of high-magnification (X400)- (selected ROIs) and low-magnification (X200)- textured meshes

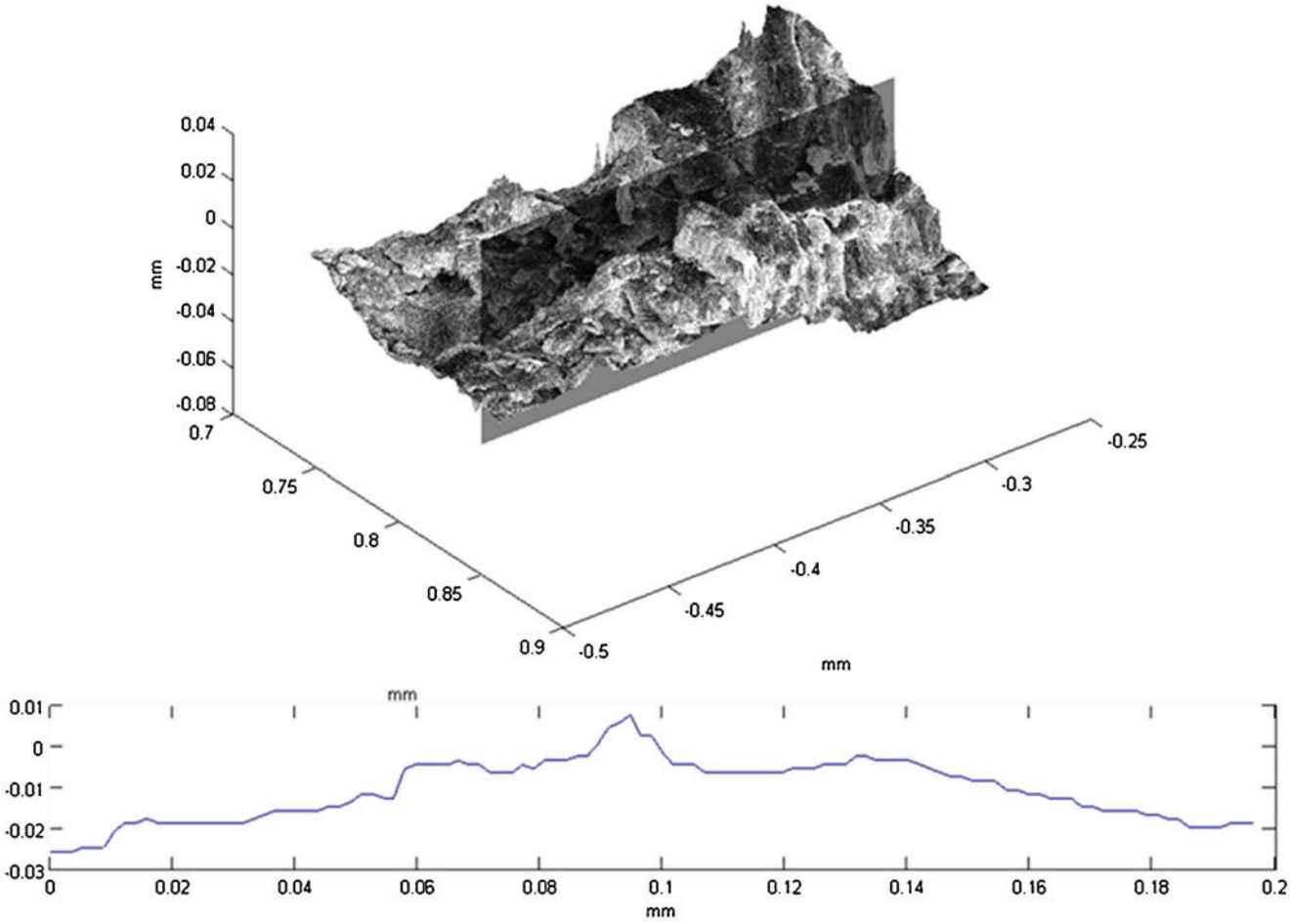

Fig. 11 Magma material x500- a textured mesh and an extracted profile

textured surface. When the images and the meshes shown in Figs. 12(c) and 13(c) are enlarged, the smooth transition between the areas of the optical and digital zooming is clearly evident. Again the 3D features can be easily identified.

Figure 15(a) shows images from *a brittle material*. Again there is a smooth transition between the areas of the optical and the digital zooming. As expected, the optical zooming provides more details relative to the digital zooming. The features can be identified clearly at different scales. Figure 15

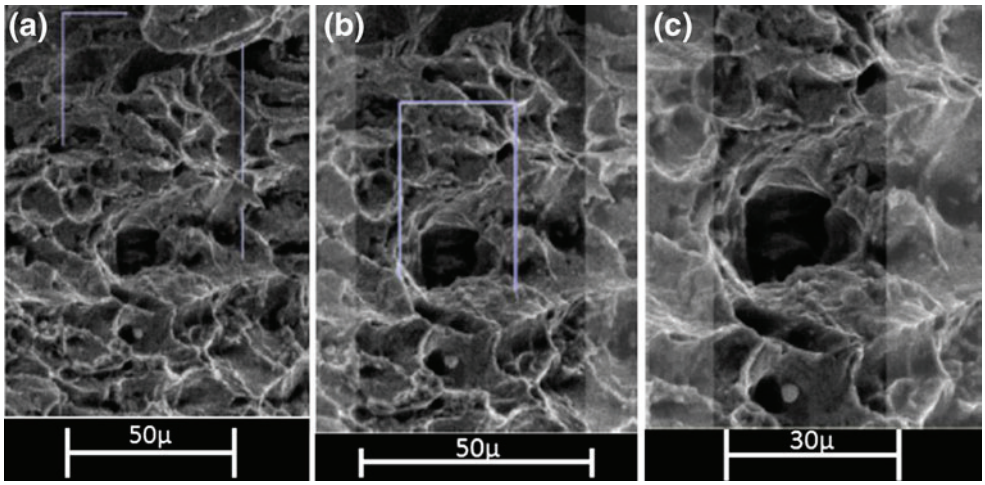

Fig. 12 Ductile steel fractured surface: Zooming of an image (**a**)–(**c**)

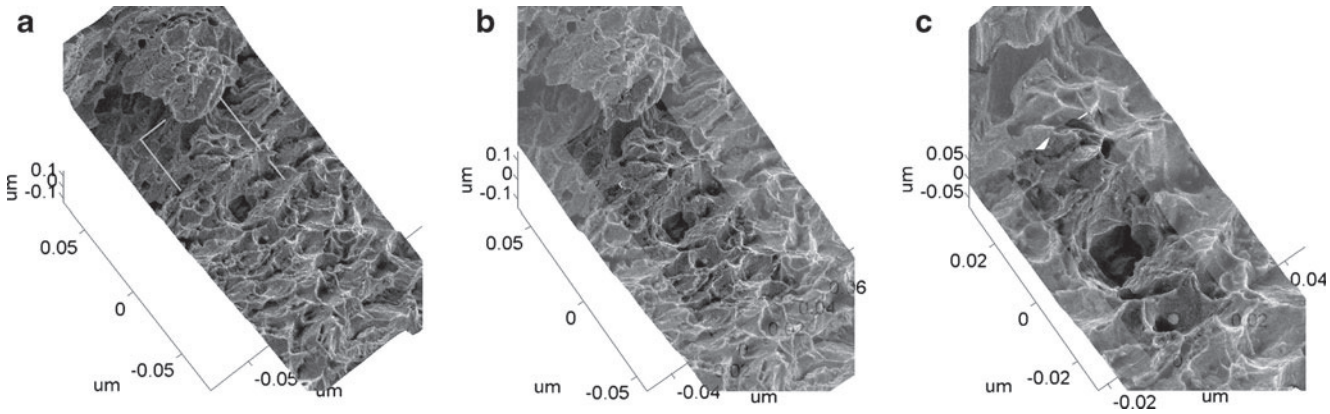

Fig. 13 Ductile steel fractured surface- Zooming of the textured mesh (**a**)–(**c**)

(b) and (c) show the image and the 3D textured mesh of *brittle material* at a zoom of x800. Figure 15(d) and (e) show the image and 3D textured mesh of *brittle steel* at a zoom of x1600. In this example as well, there is a

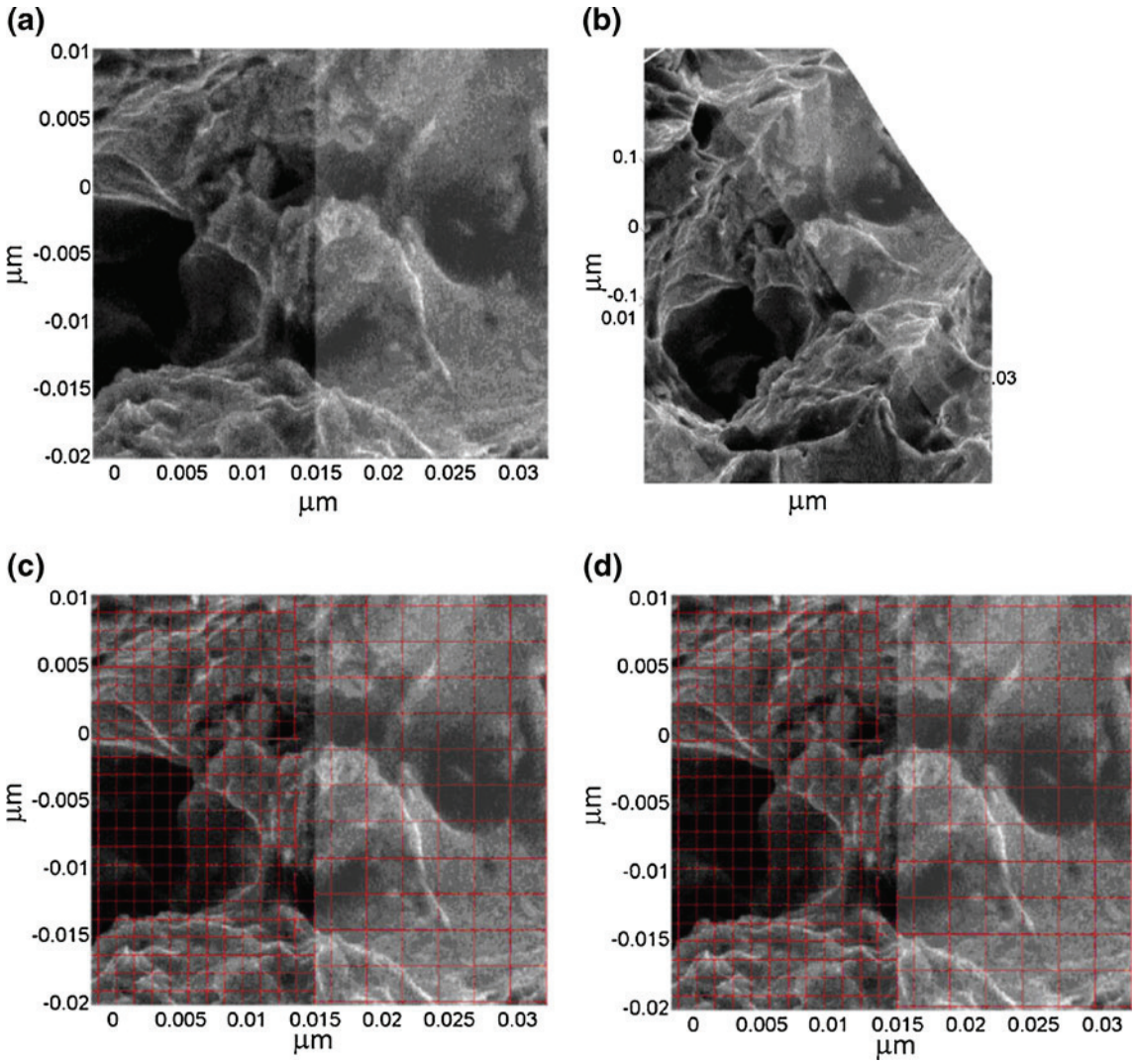

Fig. 14 Ductile steel fractographs x3200. The light and the dark areas represent the digital and optical zooming respectively: (**a**)–(**b**) The image and textured mesh with the digital and optical zooming; (**c**)–(**d**) The mesh (red grid) is demonstrated on the image and the textured mesh with the digital and optical zooming

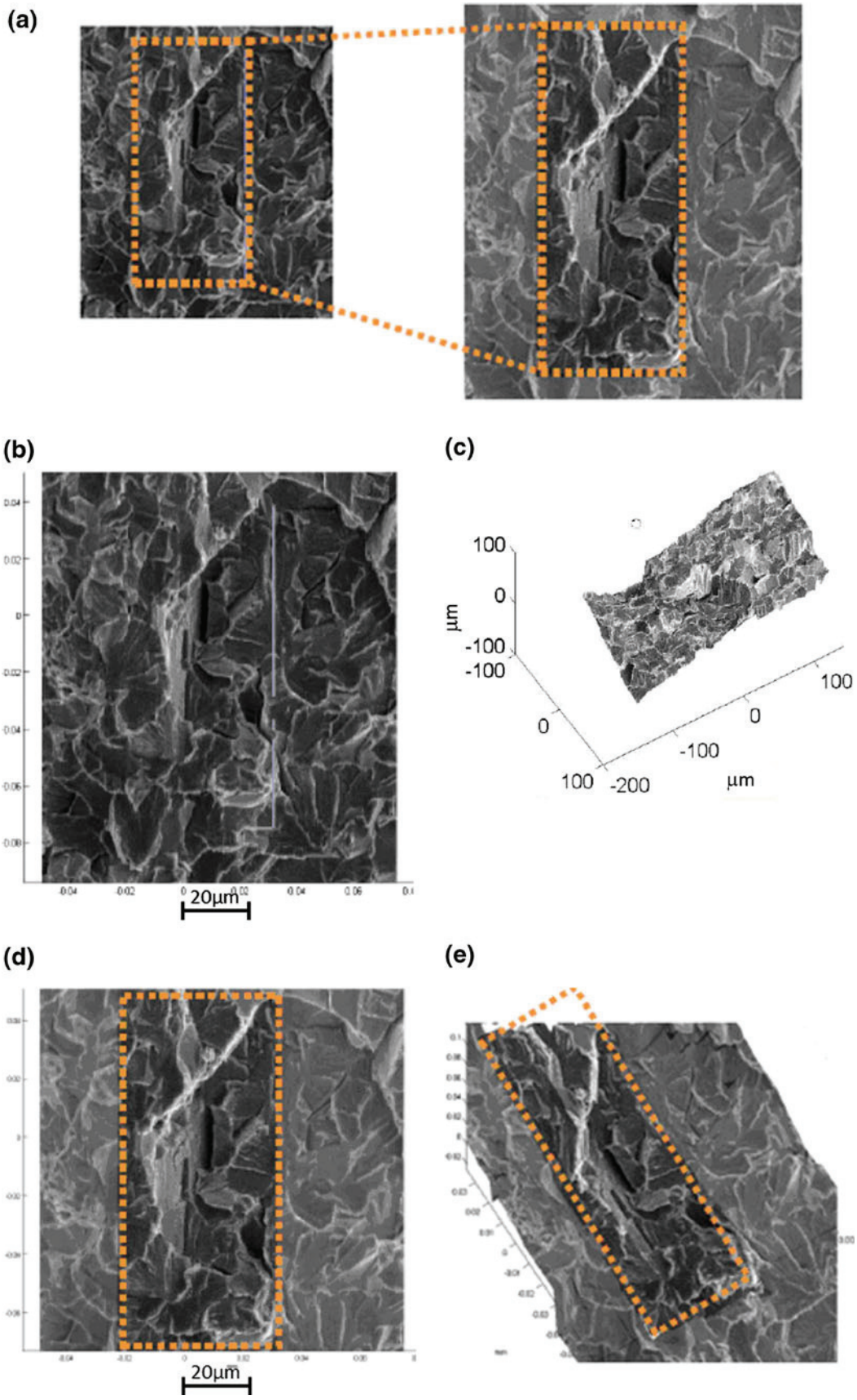

Fig. 15 Brittle steel fractographs: (**a**) Image zooming - x800 and x1600; an image and a textured mesh: (**b**)–(**c**) x800; (**d**)–(**e**) x1600

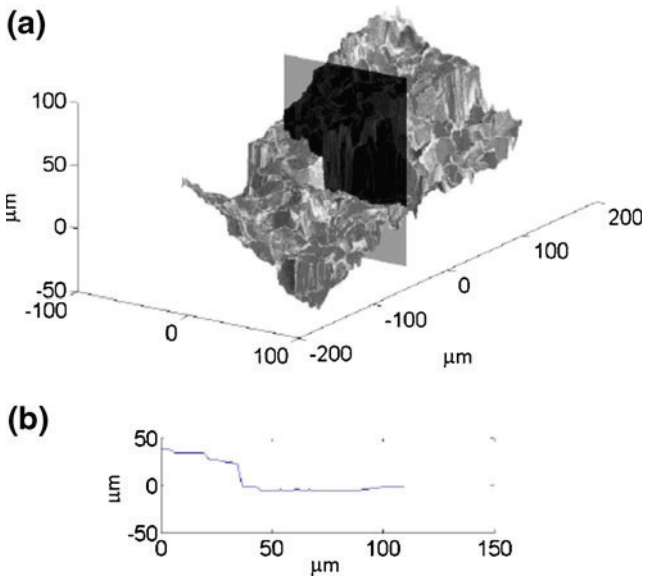

Fig. 16 Brittle steel x1600: (**a**) a textured mesh and the profile plane; (**b**) the profile

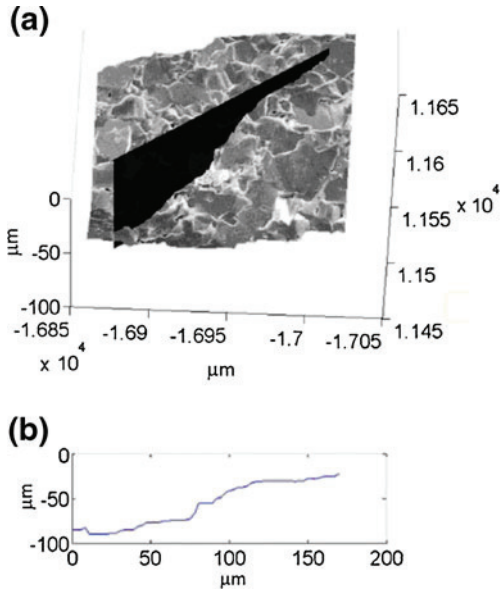

Fig. 18 Magma x500: (**a**) a textured mesh and the profile plane; (**b**) the profile

smooth transition between the areas of the optical and digital zooming, and the 3D features can be identified clearly at different scales.

Examples: Profiles Extracted from Textured Meshes

Extraction of a profile from a textured mesh in a given direction was tested on several material samples, and the images were scanned at different scales. The method is demonstrated on samples of *brittle steel* (x1600), Tungsten heavy alloy (x800), Magma (x500) and 99.5% aluminum (x400). Figures 15, 16, 17, 18 and 19 show the textured mesh and a plane (upper figure), where the plane represents the pre-defined direction. The resulting profile is obtained by intersecting the plane and the textured mesh (lower figure). With the proposed system the direction of a profile can be defined interactively. Verification of the digital profile with a measured profile is beyond the scope of this paper.

The proposed method has been demonstrated on several samples. The performance of the resulting multi-scale model has been analyzed for each sample on each scale separately.

In our examples, we decided to compromise by using the smallest tilt angle possible to process the data (5 deg is adequate for that purpose), since larger angles will result in a loss of focus and/or depth of field. While this can be corrected on most SEMs, we did not want to induce optical preconditioning of that kind to the raw data.

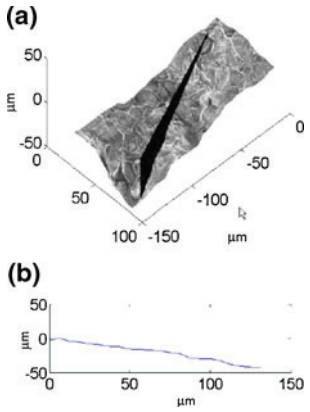

Fig. 17 Tungsten heavy alloy x800: (**a**) a textured mesh and the profile plane; (**b**) the profile

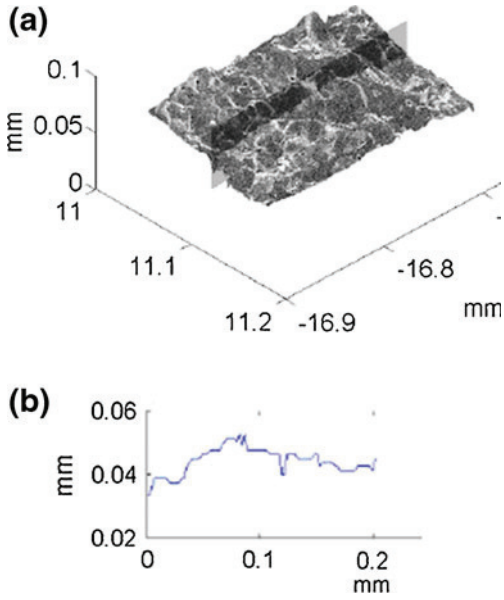

Fig. 19 99.5% aluminum x400: (**a**) a textured mesh and the profile plane; (**b**) the profile

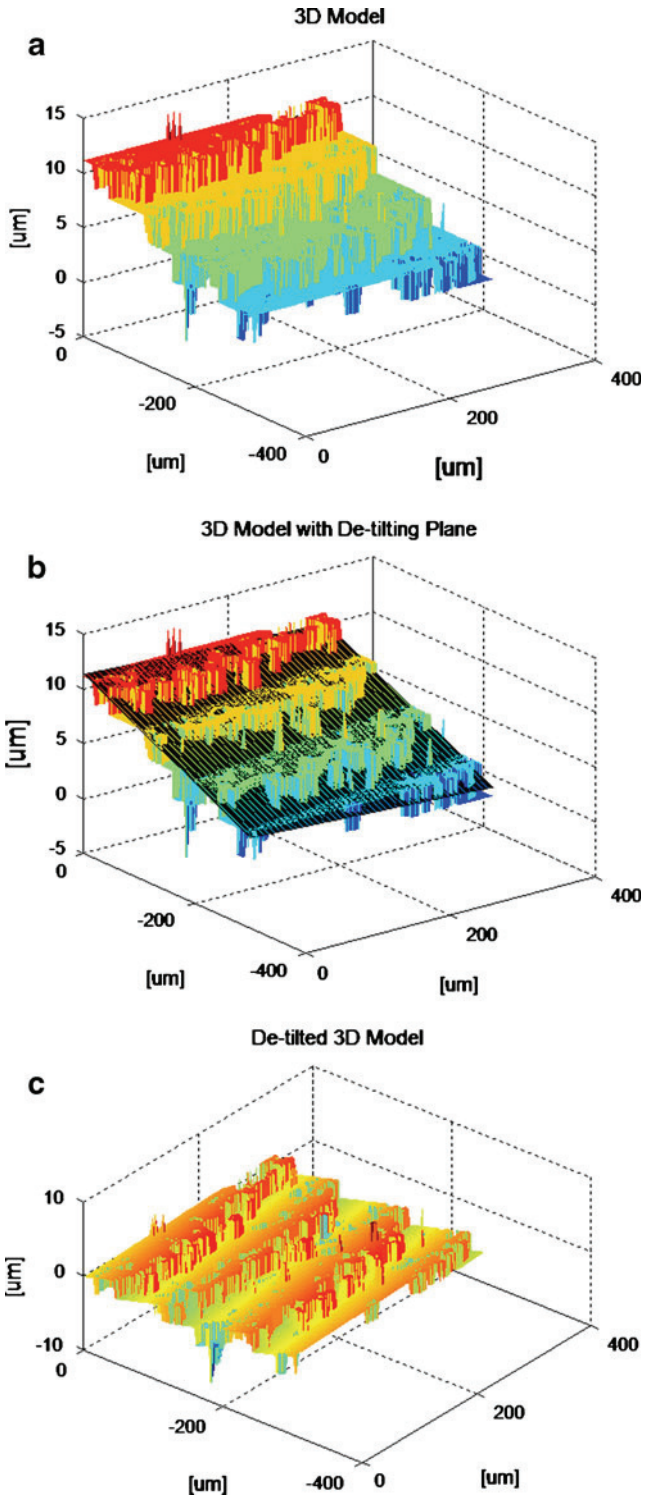

Fig. 20 Roughness results measured using multi-scale photogrammetric SEM system. Each sub-figure shows the reconstructed surface, the reconstructed surface with the plane fitted (used for detilting) and the detilted surface (used for roughness calculation): (**a**) roughness results calculated for Alumina Ra0.8 specimen with x400 magnification; (**b**) roughness results calculated for Alumina Ra0.8 specimen with x1600 magnification

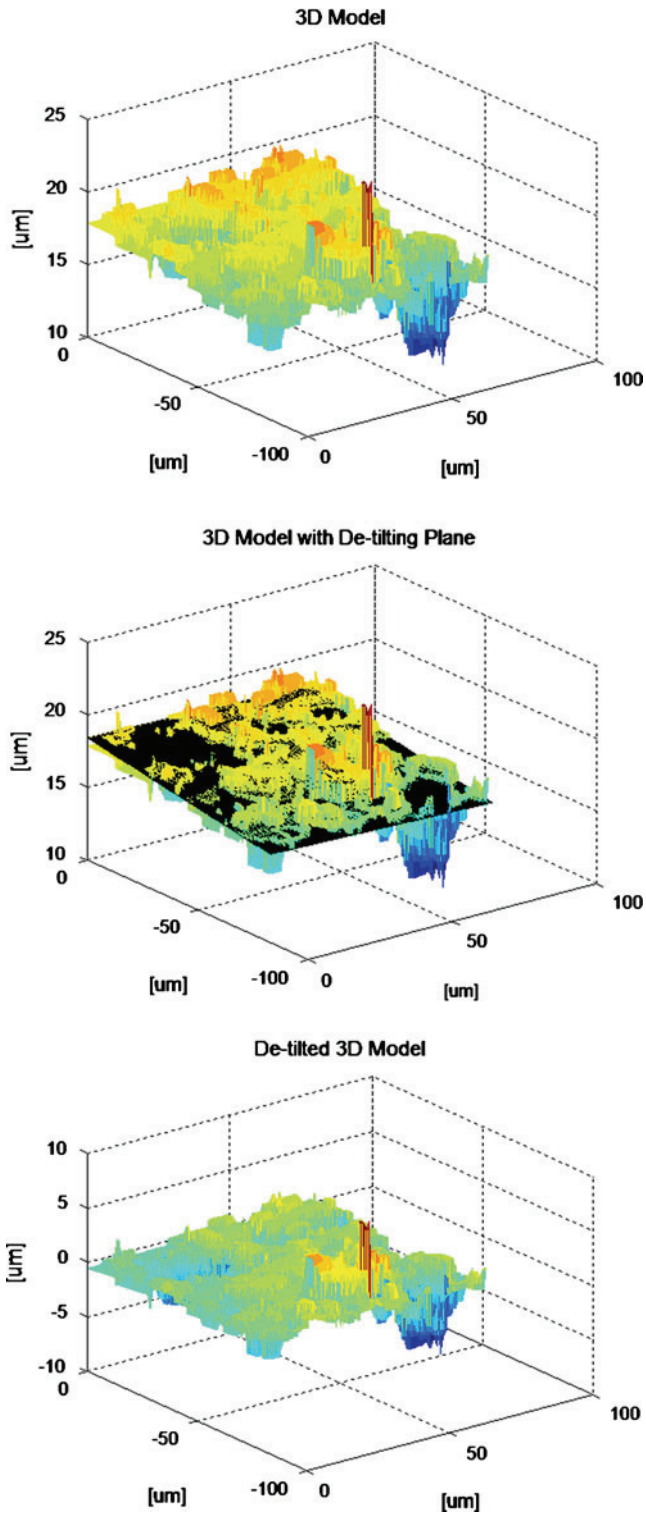

Fig. 20 (continued)

Verification: Estimation of the Accuracy of Roughness Measurements

In order to validate the roughness results measured on Multi-scale Stereo-Photogrametric SEM System, we performed roughness measurements for the analyzed specimen, using optical profilometry (Wyko NT1100 optical interferometer, Veeco, USA) on a polished alumina sample. The surface roughness Sa measured in optical profilometer was Sa=0.8 μ. In Multi-scale Stereo-Photogrametric SEM, two scales were used for the evaluation, namely x400 (300×300 μ field of view on specimen) and x1600 (70×70 μ field of view on specimen). Since, some tilt to the specimen was introduced to the tested specimen during measurement, the reconstructed 3D surfaces were "de-tilted" by subtracting a fitted plane to the resulted 3D surface. Then, the roughness Sa was subsequently calculated according to the following formula:

$$S_a = \frac{1}{n}\sum_{i=1}^{n}|y_i|$$

A comparison of the results is shown in Fig. 20. For the lower magnification, we obtained Sa=0.8851 μ, while for the higher magnification, we measured Sa=0.8395 μ.

It is important to note in passing that a crucial limitation of the optical profilometer is that it cannot perform roughness measurement on fracture surfaces, while the presented method allows for such measurements, for which no direct comparison is possible at that stage.

The results of this comparison show an excellent match for the roughness values measured using contact profilometry and the proposed non-contact method. These results, albeit of a preliminary nature, indicate the proposed method is sufficiently accurate to provide reliable surface roughness estimates.

Summary and Conclusions

A new system for inspecting 3D fracture surfaces has been developed to visualize and analyze fracture surfaces. The main advantages of the proposed system can be summarized as follows:

- The proposed 3D multi-scale model enables analysis and visualization of fracture surfaces at different resolutions and scales (levels of detail).
- The intermediate structural levels allow seamless transition between desired levels.
- The proposed multi-scale method adaptively provides a highly detailed model suitable for qualitative and quantitative analyses, e.g. finite element analysis.
- The proposed inspection system creates a new interactive 3D digital and virtual environment by applying data fusion between the real multi-scale images and the digital computed 3D mesh.
- The profilometric analysis can be applied interactively on the textured meshes in any given direction and the 1D profiles can be subsequently analyzed.
- The 3D model will yield better insight about fracture surfaces and provide reliable and valuable feedback for engineers and scientists.
- The system roughness measurements were shown to be similar to optical profilometer roughness measurements. In addition, the system is able to conduct roughness measurements not only on polished surfaces but also on fracture surfaces.

The main limitation of the proposed system can be summarized as follows:

- The tested surfaces must have multiple unique features. Otherwise the correlation process may fail.
- High-scale surface areas are limited to small areas, since their analysis requires laborious work.
- Some manual work is needed for reconstruction. In the future, this process will likely be automated.

References

1. Torquato S (2002) Random heterogeneous materials: microstructure and macroscopic properties. Springer, New York
2. Santucci S, Toussaint R, Schmittbuhl J, Hansen A, Maløy KJ (2010) Fracture roughness scaling: A case study on planar cracks. A Letters Journal Exploring the Frontiers of Physics
3. Stampfl J et al (1996) Determination of the fracture toughness by automatic image processing. Int J Fract 78(1):35–44
4. Stampfl J et al (1996) Reconstruction of surface topographies by scanning electron microscopy for application in fracture research. Appl Phys Mater Sci Process 63(4):341–346
5. Orteu JJ et al (2011) Multiple-camera instrumentation of a single point incremental forming process pilot for shape and 3D displacement measurements: methodology and results. Exp Mech 51:625–639
6. Kolednik O, Stuwe H (1985) The stereo-photogrammetric determination of the critical crack tip opening displacement. Eng Fract Mech 1985:1145–55
7. Zhu T et al (2011) Quantitative stereovision in a scanning electron microscope. Exp Mech 51(1):97–109
8. Wang Y-Q et al (2011) On Error Assessment in stereo-based deformation measurements, Part I: theoretical developments for quantitative estimates. Exp Mech 51(4):405–422
9. Marinello F, Savio E, Horsewell A, De Chiffre L (2008) Critical factors in SEM 3D stereo microscopy. Meas Sci Tech
10. Schreier H, Garcia D, Sutton M (2004) Advances in light microscope stereo vision. Exp Mech 44(3):278–288
11. Samak D, Fischer A, Rittel D (2007) 3D reconstruction and visualization of microstructure surfaces from 2D images. CIRP Ann Manuf Technol 56(1):149–152
12. Choi B et al (1988) Triangulation of scattered date in 3D space. Comput Aided Des 20(5):239–248

13. Lorensen W, Cline H (1987) Marching cubes: a high resolution 3D surface construction algorithm. SIGGRAPH Comput Graph 21:163–169
14. Losasso F, Hoppe H (2004) Geometry clipmaps: terrain rendering using nested regular grids. ACM Trans Graph 23(3):769–776
15. Schroeder W, Shephard M (1988) Geometry-based fully automatic mesh generation and the Delaunay triangulation. Int J Numer Meth Eng 26(11):2503–2515
16. Azernikov S, Fischer A (2006) A new volume warping method for surface reconstruction. J Comput Inf Sci Eng 6(4):355–363
17. Heckbert PS (1986) Survey of texture mapping. Comput Graph Appl IEEE 6(11):56–67
18. Luebke D et al (2002) Level of detail for 3D Graphics. Morgan Kaufmann Series in Computer Graphics. San Francisco: Morgan Kaufmann: 432
19. Azernikov S, Miropolsky A, Fischer A (2003) Surface reconstruction of freeform objects based on multiresolution volumetric method. J Comput Inf Sci Eng 3(4):334–338
20. Samet H (1990) The design and analysis of spatial data structures. Addison-Wesley, Reading
21. Han C et al (2008) Multiscale texture synthesis. ACM Trans Graph 27(3):1–8
22. Zaoui A (2002) Continuum micromechanics: survey. J Eng Mech 128(8):808–816
23. Shmukler A, Fischer A (2010) Verification of 3D freeform parts by registration of multiscale shape descriptors. Int J Adv Manuf Technol 49(9):1093–1106
24. Kanade T (1994) A stereo matching algorithm with an adaptive window: theory and experiment. IEEE Trans Pattern Anal Mach Intell 16:920–932
25. Lewis J (1995) Fast normalized cross-correlation template matching by cross. Comput Inform Sci 1995(1):120–123
26. Haralick RM, Shapiro LG (1992) Computer and robot vision vol. II. Addison-Wesley, Boston
27. MathWorks (2009) Available from: www.mathworks.com/products/matlab/
28. Lorensen WE, Cline HE (1987) Marching cubes: a high resolution 3D surface construction algorithm. SIGGRAPH Comput Graph 21 (4):163–169